Duty ratio of cooperative molecular motors

Nadiv Dharan[1] and Oded Farago[1,2]

[1]*The Faculty of Engineering Sciences, Department of Biomedical Engineering*
[2]*Ilse Katz Institute for Nanoscale Science and Technology, Ben Gurion University of the Negev, Be'er Sheva IL-84105, Israel*

Molecular motors are found throughout the cells of the human body and have many different and important roles. These micromachines move along filament tracks and have the ability to convert chemical energy into mechanical work that powers cellular motility. Different types of motors are characterized by different duty ratios, which is the fraction of time that a motor is attached to its filament. In the case of myosin II (a nonprocessive molecular machine with a low duty ratio), cooperativity between several motors is essential to induce motion along its actin filament track. In this work we use statistical mechanical tools to calculate the duty ratio of cooperative molecular motors. The model suggests that the effective duty ratio of nonprocessive motors that work in cooperation is lower than the duty ratio of the individual motors. The origin of this effect is the elastic tension that develops in the filament which is relieved when motors detach from the track.

PACS number(s): 87.16.Nn, 87.16.A−, 87.16.Uv, 87.16.Ka

I. INTRODUCTION

Motor proteins are molecular machines that convert chemical energy into mechanical work by adenosine triphosphate (ATP) hydrolysis. They "walk" on the microtubule and actin cytoskeleton and pull vesicles and organelles across the cell [1]. Motor proteins can be classified into processive and nonprocessive motors. The former class includes motors like kinesins, which travel a long distance along their cytoskeleton track (microtubules) without detachment [2]. In the latter class, we find motors like myosins that make only a single step along their tracks (actin filaments) before disconnection [3]. While processive motors can move cargoes by operating individually, nonprocessive motors need to work in cooperation to generate substantial movement. The cooperative action of myosin motors is implicated in a variety of cellular processes, including the contraction of the contractile ring during cytokinesis [4], adaptation of mechanically activated transduction channels in hair cells in the inner ear [5], and muscle contraction [6]. Another important example of cooperative motor dynamics is found in motility assays, where filaments glide over a surface densely covered by motor proteins [7].

One of the more interesting outcomes of cooperative action of molecular motors is their ability to induce bidirectional motion. Bidirectional motion is observed when a filament is subjected to the action of two groups of motors that engage in a "tug-of-war" contest and exert forces in opposite directions [8]. The motor party that exerts the larger force determines the instantaneous direction of motion, which is reversed when the balance of forces shifts from one group to the other. Earlier theoretical models suggested that the characteristic reversal time of the bidirectional dynamics (i.e., the typical duration of the unidirectional intervals of motion) $\tau_{\rm rev}$ grows exponentially with the number of motors N [9]. In these earlier models, the moving filament was treated as a rigid rod which does not induce elastic coupling between the motors. A recent motility assay of myosin II motors and actin filaments with alternating polarities challenged this prediction. It was found that the characteristic reversal times of the bidirectional motion in this motility assay were macroscopically large, but practically independent of the number of motors [10]. This observation

has been explained by a model that accounts for the elasticity of the actin filament [10,11]. It has been shown that the motors indirectly interact with each other via the tensile stress that they generate in the elastic filament. The elasticity-mediated crosstalk between the motors leads to a substantial increase in their unbinding rates, making each motor effectively less processive and eliminating the exponential growth of $\tau_{\rm rev}$ with N [12].

The reduction in the duty ratio (the fraction of time that each motor spends attached to the filament track) of the cooperative motors can be explained as follows: During bidirectional motion, the elastic filament is subjected to a tug-of-war between motors that exert opposite forces, which leads to large stress fluctuations along the elastic filament. These stress fluctuations are the origin of the elasticity-mediated crosstalk effect. Detailed analysis shows that the typical elastic energy stored in the actin filament scales as [10,11]

$$\frac{E}{k_B T} = \alpha N n, \tag{1}$$

where N is the number of motors, n is the number of *connected* motors, and α is a dimensionless parameter [which is closely related to the parameter β^*, to be defined below in Eq. (3)]. For actin-myosin II systems, α is rather small (for the motility assay described by the authors of Ref. [10], $\alpha \sim 2 \times 10^{-3}$), but the energy released upon the detachment of a single motor ($n \to n-1$): $\Delta E / k_B T = -\alpha N$ can be quite large if N is large. This last result implies that for large N, the transitions of motors between the attached and detached states are influenced by both ATP-driven (out-of-equilibrium) processes as well as by thermal (equilibrium) excitations. The latter will be dominated by the changes in the elastic energy of the actin [see Eq. (1)] and not by the energy of the individual motors.

For the actin filament with alternating polarities, the elasticity-mediated crosstalk is a cooperative effect that reduces the degree of cooperativity between motors (decreases $\tau_{\rm rev}$) by decreasing their duty ratio (i.e., their attachment probability). But as discussed above, much of the strength of this effect is related to the large stress fluctuations that develop in the elastic filament due to the opposite forces applied by the
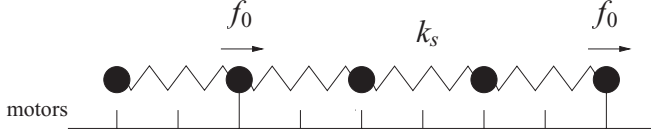
FIG. 1. The actin elastic filament is represented as a chain of nodes, connected by identical springs with spring constant k_s. Each node is either connected to a single myosin II motor, in which case it experiences a force of magnitude f_0, or disconnected, in which case it experiences no force.

antagonistic motors. In view of this fact, it is fair to question the significance of this effect in the more common situation where polar filaments move directionally under the action of a single family of motor proteins. In this work we analyze this problem and show that the elasticity-mediated crosstalk effect in this system is indeed much smaller, but not entirely negligible. Our analysis of this effect is presented in Sec. II. The magnitude of this effect in actomyosin systems is estimated in Sec. III.

II. STATISTICAL-MECHANICAL MODEL

In what follows we model the elastic actin filament as a chain of N equally spaced nodes connected by $N-1$ identical springs with spring constant k_s (see Fig. 1). In the chain reference frame, the ith node is located at $x_i = (i-1)\Delta l$, where $i = 1, \ldots, N$ and Δl is the spacing between the nodes. For brevity we set $\Delta l = 1$. The chain lies on a "bed" of motors, where each node may be either free and experience no pulling force ($f_i = 0$), or attached to one motor in which case it is subjected to a force of magnitude $f_i = f_0$. Different configurations of the system are defined according to which nodes are connected to motors and which are not. For a given configuration j, the elastic energy of the chain is given by the sum of energies of the springs $E_j^{\rm el} = \sum_{i=1}^{N-1} F_i^2/2k_s$, where F_i is the force applied on the ith spring. The forces F_i are calculated as follows. We first calculate the mean force $\bar{f} = (\sum_{i=1}^N f_i)/N$, and define the excess forces acting on the nodes $f_i^* = f_i - \bar{f}$. The force on the ith spring is then obtained by summing the excess forces applied on all the monomers located on one side of the spring: $F_i = -\sum_{l=1}^i f_l^* = \sum_{l=i+1}^N f_l^*$.

It is more convenient to analyze the problem using continuous functions. Let us introduce the function $h(x)$ which, for $x_i < x < x_{i+1}$, has a slope $+1$ if the monomer at x_i is connected to a motor, and a slope 0 otherwise. Thus, $h(x)$ gives the total force applied on the chain up to the point x, with $h(x=0) = 0$ and $h(x=N) = n$, where n is the number of monomers connected to motors in a given configuration. The solid line in Fig. 2 shows the function $h(x)$ corresponding to the configuration of five nodes depicted in Fig. 1. To calculate the elastic energy of a configuration we introduce the function $g(x) = h(x) - (n/N)x$, which is depicted by the dashed line in Fig. 2 and gives the total *excess* force accumulated up to x. The elastic energy can then be expressed as

$$\frac{E_j^{\rm el}}{k_B T} = \beta^* \sum_{i=1}^{N-1} g^2(x_i) \simeq \beta^* \int_0^N g^2(x)dx, \qquad (2)$$
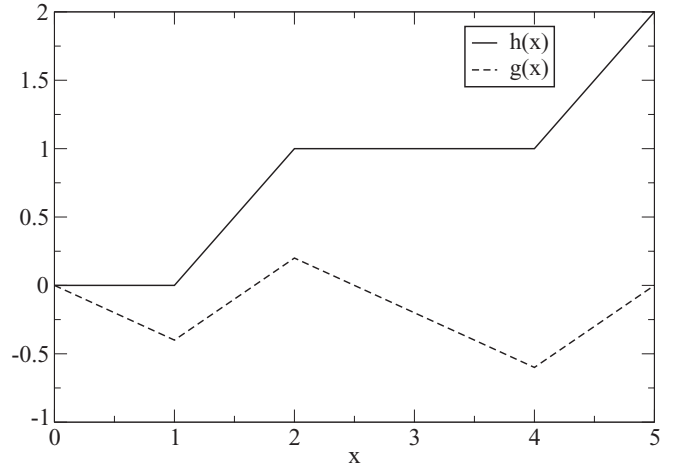

FIG. 2. The functions $h(x)$ and $g(x)$ which correspond to the configuration shown in Fig. 1.

where

$$\beta^* = \frac{f_0^2}{2k_s k_B T} \qquad (3)$$

is the ratio between the typical elastic energy of a spring $f_0^2/2k_s$ and the thermal energy $k_B T$.

To determine the mean number of connected motors, one needs to calculate the partition function

$$Z = \sum_{n=0}^N p^n(1-p)^{N-n}z_n, \qquad (4)$$

where p is the attachment probability (i.e., duty ratio) of a single motor, and z_n is the partition function of all the configurations with exactly n connected motors. The function z_n can be calculated by tracing over all the functions $g(x)$ corresponding to configurations with n connected motors. Mathematically, the condition that exactly n motors are connected can be expressed through the following constraint on the function $h(x)$

$$\lim_{\alpha \to \infty} \int_0^N \left|\frac{dh}{dx}\right|^\alpha dx = n. \qquad (5)$$

To allow an analytical solution, we approximate this constraint by setting $\alpha = 2$, in which case Eq. (5) can be expressed in terms of $g(x) = h(x) - (n/N)x$ as

$$\int_0^N \left(\frac{dg}{dx}\right)^2 dx = N\frac{n}{N}\left(1 - \frac{n}{N}\right). \qquad (6)$$

With Eq. (6), the partition function z_n is given by

$$z_n = B(n,N) \int \mathcal{D}[g(x)] \exp\left(-\beta^* \int_0^N g^2(x)dx\right)$$
$$\times \delta\left[\int_0^N \left(\frac{dg}{dx}\right)^2 dx - N\frac{n}{N}\left(1 - \frac{n}{N}\right)\right], \qquad (7)$$

where δ is Dirac's delta function. The function $B(n,N)$ is introduced in Eq. (7) to compensate for the error introduced by the approximated constraint Eq. (6). We will determine this

function through the requirement that for $\beta^* = 0$, that is, in the absence of elastic crosstalk between the motors

$$z_n|_{\beta^*=0} = \binom{N}{n} = \frac{N!}{n!(N-n)!}, \tag{8}$$

which is simply the number of ways to choose n out of N monomers.

To calculate the partition function z_n, we use the Fourier space representation of $\delta(x)$

$$\delta(x-a) = \frac{1}{2\pi i}\int_{-i\infty}^{i\infty}e^{w(x-a)}dw, \tag{9}$$

and the Fourier series of $g(x)$

$$g(x) = \sum_{k=-N/2}^{N/2-1}g_k e^{i\frac{2\pi}{N}kx}. \tag{10}$$

Substituting Eqs. (9) and (10) into Eq. (7) yields

$$\begin{aligned}z_n = {}& B(n,N)\frac{1}{2\pi i}\int_{-i\infty}^{i\infty}dw\int\mathcal{D}[g_k]\\ &\times\exp\left[wN\frac{n}{N}\left(1-\frac{n}{N}\right)\right]\\ &\times\exp\left[-\sum_k g_k^2\left(\frac{8\pi^2}{N}k^2 w + 2N\beta^*\right)\right].\end{aligned} \tag{11}$$

Tracing over g_k can be readily performed, giving

$$\begin{aligned}z_n = {}& B(n,N)\frac{1}{2\pi i}\int_{-i\infty}^{i\infty}dw\exp\left[wN\frac{n}{N}\left(1-\frac{n}{N}\right)\right]\\ &\times\left\{\prod_{k=0}^{N/2}\frac{\pi}{2N\beta^*+8\pi^2 k^2 w/N}\right\}.\end{aligned} \tag{12}$$

The integral over w can be evaluated using the method of steepest descent, which yields

$$z_n \simeq B(n,N)\,e^{G(w_0)}, \tag{13}$$

where

$$\begin{aligned}G(w) = {}& n\left(1-\frac{n}{N}\right)w - \sum_{k=0}^{N/2}\ln\left[\frac{1}{\pi}\left(\frac{8\pi^2}{N}k^2 w + 2N\beta^*\right)\right]\\ \simeq {}& N\left\{w\frac{n}{N}\left(1-\frac{n}{N}\right) - \frac{1}{2}\ln\left[\frac{2e^{-2}N}{\pi}(\pi^2 w + \beta^*)\right]\right.\\ &\left. - \sqrt{\frac{\beta^*}{\pi^2 w}}\tan^{-1}\left(\sqrt{\frac{\pi^2 w}{\beta^*}}\right)\right\},\end{aligned} \tag{14}$$

and w_0 satisfying

$$\begin{aligned}\left.\frac{dG}{dw}\right|_{w_0} = {}& \frac{n}{N}\left(1-\frac{n}{N}\right) - \frac{1}{2w_0}\\ &+ \frac{1}{2}\sqrt{\frac{\beta^*}{\pi^2 w_0^3}}\tan^{-1}\left(\sqrt{\frac{\pi^2 w_0}{\beta^*}}\right) = 0.\end{aligned} \tag{15}$$

For $\beta^* \ll 1$, one gets

$$w_0 \simeq \frac{N}{2n}\left(\frac{N}{N-n}\right) - \sqrt{\frac{N}{8n}\left(\frac{N}{N-n}\right)\beta^*}. \tag{16}$$

From Eqs. (8), (13), (14), and (16), one finds that

$$\begin{aligned}B(n,N) = {}& \binom{N}{n}e^{-G(w_0)}\bigg|_{\beta^*=0}\\ = {}& \binom{N}{n}\left(\frac{\pi}{e^3}\right)^{(N/2)}\left(\frac{N^3}{n(N-n)}\right)^{N/2}.\end{aligned} \tag{17}$$

Inserting Eq. (16) into Eq. (14), and expanding $G(w_0)$ in powers of $\sqrt{\beta^*}$, yields

$$G(w_0) \simeq G(w_0)|_{\beta^*=0} - \sqrt{\frac{n(N-n)}{2}\beta^*}. \tag{18}$$

Finally, for $\beta^* \ll 1$, the partition function z_n is obtained by substituting Eqs. (17) and (18) into Eq. (13), which gives

$$z_n \simeq \binom{N}{n}\exp\left(-\sqrt{\frac{n(N-n)}{2}\beta^*}\right). \tag{19}$$

To calculate the partition function Z, one needs to substitute Eq. (19) into Eq. (4), which gives

$$Z = \sum_{n=0}^{N}\binom{N}{n}p^n(1-p)^{N-n}\exp\left(-\sqrt{\frac{n(N-n)}{2}\beta^*}\right). \tag{20}$$

In the thermodynamic limit ($N \gg 1$), the sum in Eq. (20) is dominated by one term which corresponds to the mean number of attached motors $\langle n\rangle$. This term is given by

$$\langle n\rangle = N\left[p - (1-2p)\sqrt{\frac{p(1-p)}{8}\beta^*}\right]. \tag{21}$$

From Eq. (21) we identify the *effective* attachment probability as

$$p_{\text{eff}} \equiv \frac{\langle n\rangle}{N} = p - (1-2p)\sqrt{\frac{p(1-p)}{8}\beta^*}. \tag{22}$$

Notice that the second term on the right-hand side of Eq. (22) is antisymmetric around $p = 1/2$, and that for $p < 1/2$ ($p > 1/2$), the effective attachment probability p_{eff} is smaller (larger) than p. This observation is directly related to the fact the elasticity-mediated crosstalk effect is driven by the tendency to reduce the force fluctuations along the elastic filament. For $p < 1/2$ ($p > 1/2$) the force fluctuations are reduced by the detachment (attachment) of motors, which brings the system closer to the limiting case $p = 0$ ($p = 1$) where the force fluctuations vanish.

To test the validity and range of applicability of Eq. (22), we conducted Monte Carlo (MC) simulations of elastic chains of $N = 1000$ monomers with $p = 0.05$, which is the typical duty ratio of myosin II motors [13]. Systems corresponding to different values of β^* were simulated using the parallel tempering method. The simulations include two types of elementary moves (which are attempted with equal probability); one in which the state (connected or disconnected) of a randomly chosen node changes, and the other in which two randomly chosen nodes with opposite states change their states simultaneously. For each move attempt, the model energy of the chain is recalculated, and the move is accepted or rejected according to the conventional Metropolis criterion. Our MC results are summarized in Fig. 3. For $\beta^* < 0.2$, we find an excellent agreement between our computational results and Eq. (22) (which has been derived for $\beta^* \ll 1$). Notice that
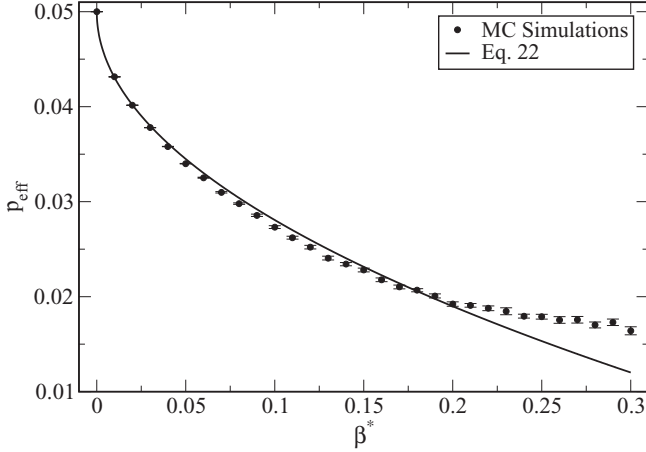
FIG. 3. The effective attachment probability as a function of the dimensionless parameter β^*. The circles denote the results of the MC simulations, while the solid line depicts the analytical approximation for $\beta^* \ll 1$, Eq. (22).

Eq. (22) does not include *any* fitting parameters. For larger values of β^*, Eq. (22) overestimates the decrease in p_{eff}.

III. ACTIN-MYOSIN II SYSTEMS

Equation (3) relates the dimensionless parameter β^* to three physical parameters of the system: the temperature T, the typical force exerted by the motors f_0, and the effective spring constant of the actin filaments segment between two binding sites of the motors k_s. The last parameter can be further expressed as

$$k_s = \frac{YA}{l},$$ (23)

where Y is Young's modulus of the actin, A is the cross-sectional area of an actin filament, and l is the distance between binding sites. For myosin II motors, forces in the range of $f_0 = 5-10$ pN have been measured experimentally [13,14]. The actin-cross sectional area (including the tropomyosin wrapped around the actin helix) is $A = 23$ nm^2, and the Young's modulus of the actin-tropomyosin filament is $Y = 2.8$ GPa [15,16]. The value of l is somewhat more difficult to assess. One possibility is that $l \simeq 5.5$ nm, which is simply the size of the G-actin monomers, each of which includes one binding site for myosin motors [17]. Another possible value is related to the double helical structure of F-actin and the fact that it completes half a twist about every seven monomers (i.e., every $\simeq 38$ nm [18]). Since the binding sites follow a twisted spatial path along the double helix, many of them remain spatially unavailable to the motors. In the motility assay, the motors are located underneath the F-actin, and the distance between the binding sites along the line of contact with the bed of motors is $l = 38$ nm. A third choice for l, which may be more relevant to skeletal muscles, is $l = 14$ nm. This value is derived from the fact that within the sarcomere (the basic contractile unit of the muscle) an average number of three thick myosin filaments surround one thin actin filament. The separation between collinear motor heads along the thick filament is ~ 43 nm [19–21], and because the actin is surrounded by three

thick filaments, the distance between the motors *along the actin* is $l = 43/3 \simeq 14$ nm.

For the duty ratio p, the range of experimental values is scattered and varies from $p = 0.01-0.02$ [22] to $p = 0.05$ [13]. The uncertainty may be partially related to the elasticity cross-talk effect discussed here. It also stems from the fact that p also depends on the distance and orientation of the motor head (both in space and time) with respect to the associated binding site. These may vary between the motors which, hence, should have different attachment probabilities [23].

Using the above-mentioned values of system parameters, one finds that for actomyosin systems the parameter β^* lies within the range of $5 \times 10^{-4} \lesssim \beta^* \lesssim 5 \times 10^{-3}$. Setting the duty ratio of myosin II to $p = 0.05$ (as used in the MC simulations) we find that for this range of β^*, the *effective* duty ratio is slightly lower than p and lies within the range of $p_{\text{eff}} = 0.97p$ (for $\beta^* = 5 \times 10^{-4}$) and $p_{\text{eff}} = 0.90p$ (for $\beta^* = 5 \times 10^{-3}$). Using a lower estimate for the duty ratio $p = 0.02$ [22], we find that the effective duty ratio drops to $0.83p \lesssim p_{\text{eff}} \lesssim 0.95p$ for the same range of β^*.

As stated earlier, the cooperative action of myosin motors "compensates" for the nonprocessive character of the individual motors. The force generated by a group of N motors is $\langle F \rangle = Np_{\text{eff}}f_0$. Which force f_0 maximizes the effective force per motor $f_{\text{eff}} = \langle F \rangle / N$ and, hence, the force production of the collectively working motors? From Eqs. (3) and (22) we find that the maximum value of f_{eff} is achieved when the force of the individual motors is

$$f_0^{\text{max}} = \frac{2p}{1-2p}\sqrt{\frac{k_s k_B T}{p(1-p)}}.$$ (24)

Setting the values of the system parameters as above ($Y = 2.8$ GPa, $A = 23$ nm^2, $l = 38$ nm) and taking $p = 0.02$ as the duty ratio of a single motor, we find that $f_0^{\text{max}} \simeq 25$ pN, for which $f_{\text{eff}} \simeq 0.25$ pN. For forces in the range of $f_0 \simeq 5-10$ pN, which are typically measured for myosin II motors [13], the effective mean force per motor is $f_{\text{eff}} \simeq 0.1-0.15$ pN, which is about half of the optimal effective force $f_{\text{eff}}(f_0^{\text{max}})$. We thus conclude that mysoin II motors work quite close to conditions that maximize their cooperative force generation.

IV. DISCUSSION

There has recently been a considerable interest in the collective behavior of molecular motors, especially in relation to cooperative dynamics of cytoskeletal filaments in motility assays. Most studies have focused on the bidirectional motion arising when the filament is driven by two groups of antagonistic motors, or in the case when one motor party works against an external force. The present work is motivated by our recent studies of bidirectional motion in actomyosin motility assays which demonstrated that the duty ratio of the motors (and, hence, the level of cooperativity between them) is reduced by the elasticity of the actin backbone. In this paper we extended our studies to motility assays in which similar motors act on a polar actin filament without a counter external force. To single out the filament elasticity crosstalk from other possible collective effects (e.g., those associated with nonequilibrium ATP-assisted processes and with the elasticity of the motors

themselves [24–26]), we neglect motor-to-motor variations and use a model in which the motors are characterized by two mean quantities: their attachment probability to a rigid (nonelastic) filament p, and the mean applied pulling force f_0. We expect this mean-field description of the motors to hold when the number of motors N becomes large. We calculate the attachment probability to the elastic filament $p_{\text{eff}} < p$ from the partition function associated with the filament elastic energy. The elastic energy of a filament can be treated as an equilibrium degree of freedom (of a system which is inherently out-of-equilibrium) because the mechanical response of the filament to the attachment or detachment of motors occurs on time scales which are far shorter than the typical attachment time of the motors. (See the discussion in Ref. [12]. The assumption that the actin filament is in mechanical equilibrium is also made in theoretical studies of intracellular cargo transport [8] and muscle contraction [27].) Our calculation shows that p_{eff} is only slightly smaller than p. This result is very different from our previous findings for motility assays of bidirectional motion, where the elasticity-mediated crosstalk effect is substantial. Finally, we note that, although in both this and previous studies we found that $p_{\text{eff}} < p$ [11,28], the opposite relation cannot be excluded under certain conditions (e.g., when the filament experiences external forces as in single molecule experiments or muscle contraction). We intend to address this opposite scenario in a future publication, in which we investigate the variations in both p (the ATP-hydrolysis related attachment probability) and p_{eff} (which also includes the contribution due to the elastic crosstalk effect) with the muscle contraction velocity.

ACKNOWLEDGMENTS

We thank Anne Bernheim and Sefi Givli for useful discussions.

APPENDIX: ELASTIC ENERGY

We model the actin filament as a linear chain of identical particles of mass m connected by elastic (massless) springs with spring constant k_s (see Fig. 4). Three types of forces are exerted on the particles: (i) the motor forces f_i^{motor}, (ii) the spring forces F_i, and (iii) friction drag forces f_i^{drag}. Because the motion is highly overdamped, the total instantaneous force on each mass vanishes. For the ith mass, the equation of motion is

$$f_i^{\text{motor}} - f_i^{\text{drag}} + F_i - F_{i-1} = 0, \qquad \text{(A1)}$$

with $F_0 = F_N = 0$. The drag force includes two contributions; one is due to motor friction (MF) f_i^{MF} and the other due to friction with the viscous medium f_i^{viscous}. The motor
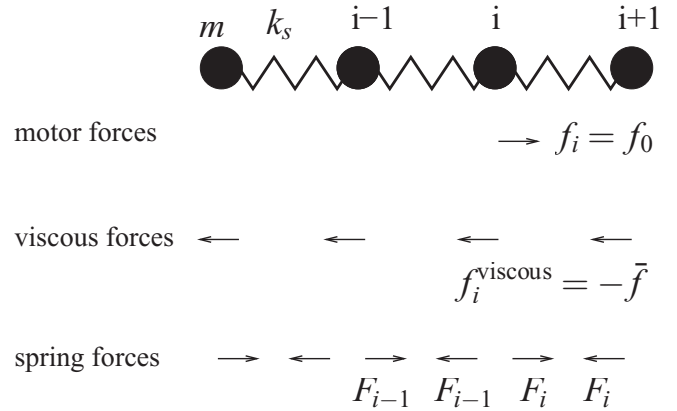

FIG. 4. The actin is modeled as a chain of masses and springs that moves in a highly viscous medium. Three types of forces are present in the system: the motor forces, a uniform viscous drag, and the spring forces. The motion is highly overdamped (zero acceleration) and thus the net force on each mass vanishes.

friction forces act only on the particles which are connected to the motors. Therefore, by redefining the motor forces $f_i = f_i^{\text{motor}} - f_i^{\text{MF}}$, we can rewrite Eq. (A1) as

$$f_i - f_i^{\text{viscous}} + F_i - F_{i-1} = 0. \qquad \text{(A2)}$$

For the chain's center of mass (c.m.), the equation of motion reads

$$F^{\text{c.m.}} = \sum_{i=1}^{N} f_i - \sum_{i=1}^{N} f_i^{\text{viscous}} = 0, \qquad \text{(A3)}$$

but the viscous drag force is distributed uniformly along the chain (i.e., it is equal for all masses) and therefore Eq. (A3) gives

$$f_i^{\text{viscous}} = \frac{\sum_{i=1}^{N} f_i}{N} = \bar{f}. \qquad \text{(A4)}$$

Using this last result, Eq. (A2) reads

$$F_i - F_{i-1} = -f_i^*, \qquad \text{(A5)}$$

where f_i^* is the excess force. Since $F_0 = 0$, we find that $F_1 = -f_1^*$. Then, $F_2 = F_1 - f_2^* = -f_1^* - f_2^*$ and, in general,

$$F_i = -\sum_{i=1}^{N} f_i^*. \qquad \text{(A6)}$$

If the motion is only partially overdamped (including in the limit of no friction), all the masses move together at the same acceleration. One can repeat the above calculation and show that Eq. (A6) remains valid.

---

[1] B. Alberts, D. Bray, J. Lewis, M. Raff, K. Roberts, and J. D. Watson, *Molecular Biology of the Cell* (Garland, New York, 1994).

[2] H. Miki, Y. Okada, and N. Hirokawa, Trends Cell Biol. **15**, 467 (2005).

[3] *Myosins: A Superfamily of Moleculare Motors*, edited by L. M. Coluccia (Springer, Dordrecht, The Netherlands, 2008).

[4] B. Feierbach and F. Chang, Curr. Opin. Microbiol. **4**, 713 (2001).

[5] E. A. Stauffer, J. D. Scarborough, M. Hirono, E. D. Miller, K. Shah, J. A. Mercer, J. R. Holt, and P. G. Gillespie, Neuron **47**, 541 (2005).

[6] M. A. Geeves and K. C. Holmes, Annu. Rev. Biochem. **68**, 687 (1999).

[7] S. J. Kron and J. A. Spudich, Proc. Natl. Acad. Sci. USA **83**, 6272 (1986).

[8] M. J. I. Müller, S. Klumpp, and R. Lipowsky, Proc. Natl. Acad. Sci. USA **105**, 4609 (2008).

[9] M. Badoual, F. Jülicher, and J. Prost, Proc. Natl. Acad. Sci. USA **99**, 6696 (2002).

[10] B. Gilboa, D. Gillo, O. Farago, and A. Bernheim-Groswasser, Soft Matter **5**, 2223 (2009).

[11] D. Gillo, B. Gur, A. Bernheim-Groswasser, and O. Farago, Phys. Rev. E **80**, 021929 (2009).

[12] O. Farago and A. Bernheim-Groswasser, Soft Matter **7**, 3066 (2011).

[13] J. T. Finer, R. M. Simmons, and J. A. Spudich, Nature (London) **368**, 113 (1994).

[14] J. E. Molloy, J. E. Burns, J. Kendrick-Jones, R. T. Tregear, and D. C. S. White, Nature (London) **378**, 209 (1995).

[15] H. Higuchi, T. Yanagida, and Y. E. Goldman, Biophys. J. **69**, 1000 (1995).

[16] H. Kojima, A. Ishijima, and T. Yanagida, Proc. Natl. Acad. Sci. USA **91**, 12962 (1994).

[17] K. C. Holmes, D. Popp, W. Gebhard, and W. Kabsch, Nature (London) **347**, 44 (1990).

[18] S. L. Hooper, K. H. Hobbs, and J. B. Thuma, Prog. Neurobiol. **86**, 72 (2008).

[19] H. E. Huxley, A. Stewart, H. Sosa, and T. Irving, Biophys. J. **67**, 2411 (1994).

[20] K. Wakabayashi, Y. Sugimoto, H. Tanaka, Y. Ueno, Y. Takezawa, and Y. Amemiya, Biophys. J. **67**, 2422 (1994).

[21] T. L. Daniel, A. C. Trimble, and P. B. Chase, Biophys. J. **74**, 1611 (1998).

[22] J. Howard, *Mechanics of Motor Proteins and the Cytoskeleton* (Sinauer, Sunderland, MA, 2001).

[23] In our statistical-mechanical analysis, p represents the typical duty ratio of individual myosin II motors, which are all assumed to have the same fixed p. It is possible that accounting for the variations in p in the model will result in a slight increase in the magnitude of the elasticity cross talk effect.

[24] K. Kruse and D. Riveline, Curr. Top. Dev. Biol. **95**, 67 (2011).

[25] T. Guérin, J. Prost, P. Martin, and J.-F. Joanny, Curr. Opin. Ceel Biol. **22**, 14 (2010).

[26] S. Banerjee, M. C. Marchetti, and K. Müller-Nedebock, Phys. Rev. E **84**, 011914 (2011).

[27] T. A. J. Duke, Proc. Nat. Acad. Sci. USA **96**, 2770 (1999).

[28] B. Gur and O. Farago, Phys. Rev. Lett. **104**, 238101 (2010).